

KLEVER

An experiment to measure $\text{BR}(K_L \rightarrow \pi^0 \nu \bar{\nu})$ at the CERN SPS

Abstract

Precise measurements of the branching ratios for the flavor-changing neutral current decays $K \rightarrow \pi \nu \bar{\nu}$ can provide unique constraints on CKM unitarity and, potentially, evidence for new physics. It is important to measure both decay modes, $K^+ \rightarrow \pi^+ \nu \bar{\nu}$ and $K_L \rightarrow \pi^0 \nu \bar{\nu}$, since different new physics models affect the rates for each channel differently. The goal of the NA62 experiment at the CERN SPS is to measure the BR for the charged channel to within 10%. For the neutral channel, the BR has never been measured. We are designing the KLEVER experiment to measure $\text{BR}(K_L \rightarrow \pi^0 \nu \bar{\nu})$ to $\sim 20\%$ using a high-energy neutral beam at the CERN SPS starting in Run 4. The boost from the high-energy beam facilitates the rejection of background channels such as $K_L \rightarrow \pi^0 \pi^0$ by detection of the additional photons in the final state. On the other hand, the layout poses particular challenges for the design of the small-angle vetoes, which must reject photons from K_L decays escaping through the beam exit amidst an intense background from soft photons and neutrons in the beam. Background from $\Lambda \rightarrow n \pi^0$ decays in the beam must also be kept under control. We present findings from our design studies for the beamline and experiment, with an emphasis on the challenges faced and the potential sensitivity for the measurement of $\text{BR}(K_L \rightarrow \pi^0 \nu \bar{\nu})$.

Input to the 2020 update of the European Strategy for Particle Physics

The KLEVER Project

F. Ambrosino,¹ R. Ammendola,² A. Antonelli,³ K. Ayers,⁴ D. Badoni,² G. Ballerini,⁵
L. Bandiera,⁶ J. Bernhard,⁷ C. Biino,⁸ L. Bomben,⁵ V. Bonaiuto,² A. Bradley,^{4,a}
M.B. Brunetti,^{1,b} F. Bucci,⁹ A. Cassese,⁹ R. Camattari,⁶ M. Corvino,¹ D. De Salvador,¹⁰
D. Di Filippo,^{1,c} M. van Dijk,⁷ N. Doble,¹¹ R. Fantechi,¹¹ S. Fedotov,¹² A. Filippi,⁸
F. Fontana,¹³ L. Gatignon,⁷ G. Georgiev,¹⁴ A. Gerbershagen,⁷ A. Gianoli,⁶ E. Imbergamo,
K. Kampf,¹⁵ M. Khabibullin,¹² S. Kholodenko,¹⁶ A. Khotjantsev,¹² V. Kozuharov,¹⁴
Y. Kudenko,¹² V. Kurochka,¹² G. Lamanna,¹¹ M. Lenti,⁹ L. Litov,¹⁴ E. Lutsenko,⁵ T. Maiolino,⁶
I. Mannelli,¹⁷ S. Martellotti,³ M. Martini,¹³ V. Mascagna,⁵ A. Maslenskina,¹² P. Massarotti,¹
A. Mazzolari,⁶ E. Menichetti,⁸ O. Mineev,¹² M. Mirra,¹ M. Moulson,³ I. Neri,⁶ M. Napolitano,¹
V. Obraztsov,¹⁶ A. Ostankov,¹⁶ G. Paoluzzi,² F. Petrucci,⁶ M. Prest,⁵ M. Romagnoni,⁶
M. Rosenthal,⁷ P. Rubin,⁴ A. Salamon,² G. Salina,² F. Sargeni,² V. Semenov,^{16,†} A. Shaykhiev,¹²
A. Smirnov,¹² M. Soldani,⁵ D. Soldi,⁸ M. Sozzi,¹¹ V. Sugoniaev,¹⁶ A. Sytov,⁶ E. Vallazza,¹⁸
R. Volpe,^{9,d} R. Wanke,¹⁹ N. Yershov¹²

¹University and INFN Naples, Italy

²University and INFN Rome Tor Vergata, Italy

³INFN Frascati National Laboratories, Italy

⁴George Mason University, Fairfax VA, USA

⁵University of Insubria, Como, Italy

⁶University and INFN Ferrara, Italy

⁷CERN EN-EA-LE, Geneva, Switzerland

⁸University and INFN Turin, Italy

⁹University and INFN Florence, Italy

¹⁰University of Padua and INFN Legnaro National Laboratories, Italy

¹¹University and INFN Pisa, Italy

¹²Institute for Nuclear Research, Moscow, Russia

¹³Marconi University and INFN Frascati National Laboratories, Italy

¹⁴University of Sofia, Bulgaria

¹⁵Charles University, Prague, Czech Republic

¹⁶Institute for High Energy Physics, Protvino, Russia

¹⁷Scuola Normale Superiore and INFN Pisa, Italy

¹⁸INFN Milano Bicocca, Italy

¹⁹University of Mainz, Germany

^aNow at Qrypt Inc., New York, USA

^bNow at University of Birmingham, UK

^cNow at Antaresvision SpA, Parma, Italy

^dNow at Université Catholique de Louvain, Belgium

[†]Deceased

Contact: Matthew Moulson, moulson@lnf.infn.it

1 Scientific context

The branching ratios (BRs) for the decays $K \rightarrow \pi \nu \bar{\nu}$ are among the observables in the quark-flavor sector most sensitive to new physics. The Standard Model (SM) rates for these flavor-changing neutral-current decays are very strongly suppressed by the GIM mechanism and the CKM hierarchy. In addition, because of the dominance of the diagrams with top loops, the lack of contributions from intermediate photons, and the fact that the hadronic matrix element can be obtained from K_{e3} data, the SM rates can be calculated very precisely: $\text{BR}(K^+ \rightarrow \pi^+ \nu \bar{\nu}) = (8.4 \pm 1.0) \times 10^{-11}$ and $\text{BR}(K_L \rightarrow \pi^0 \nu \bar{\nu}) = (3.4 \pm 0.6) \times 10^{-11}$, where the uncertainties are dominated by the external contributions from V_{cb} and V_{ub} and the non-parametric theoretical uncertainties are about 3.5% and 1.5%, respectively [1].

Because these decays are strongly suppressed and calculated very precisely in the SM, their BRs are potentially sensitive to mass scales of hundreds of TeV, surpassing the sensitivity of B decays in most SM extensions [2]. Observations of lepton-flavor-universality-violating phenomena are mounting in the B sector [3]. Most explanations for such phenomena predict strong third-generation couplings and thus significant changes to the $K \rightarrow \pi \nu \bar{\nu}$ BRs through couplings to final states with τ neutrinos [4]. Measurements of the $K \rightarrow \pi \nu \bar{\nu}$ BRs are critical to interpreting the data from rare B decays, and may demonstrate that these effects are a manifestation of new degrees of freedom such as leptoquarks [5, 6].

The BR for the charged decay $K^+ \rightarrow \pi^+ \nu \bar{\nu}$ has been measured by Brookhaven experiment E787 and its successor, E949, using K^+ decays at rest. The combined result from the two generations of the experiment, obtained with seven candidate events, is $\text{BR}(K^+ \rightarrow \pi^+ \nu \bar{\nu}) = 1.73^{+1.15}_{-1.05} \times 10^{-10}$ [7]. The goal of the NA62 experiment at the CERN SPS is to measure $\text{BR}(K^+ \rightarrow \pi^+ \nu \bar{\nu})$ to within 10% [8]. NA62 has recently obtained the result $\text{BR}(K^+ \rightarrow \pi^+ \nu \bar{\nu}) < 14 \times 10^{-10}$ (95% CL), with one observed candidate event, 0.267 expected signal events, and $0.15^{+0.09}_{-0.03}$ expected background events [9]. This result is based on 2% of the combined data from running in 2016–2018. Additional running is contemplated for 2021–2022.

The BR for the decay $K_L \rightarrow \pi^0 \nu \bar{\nu}$ has never been measured. Up to small corrections, considerations of isospin symmetry lead to the model-independent bound $\Gamma(K_L \rightarrow \pi^0 \nu \bar{\nu})/\Gamma(K^+ \rightarrow \pi^+ \nu \bar{\nu}) < 1$ [10]. Thus the 90% CL limit $\text{BR}(K^+ \rightarrow \pi^+ \nu \bar{\nu}) < 3.35 \times 10^{-10}$ from E787/E949 implies $\text{BR}(K_L \rightarrow \pi^0 \nu \bar{\nu}) < 1.46 \times 10^{-9}$.

Because the amplitude for $K^+ \rightarrow \pi^+ \nu \bar{\nu}$ has both real and imaginary parts, while the amplitude for $K_L \rightarrow \pi^0 \nu \bar{\nu}$ is purely imaginary, the decays have different sensitivity to new sources of CP violation. Measurements of both BRs would therefore be extremely useful not only to uncover evidence of new physics in the quark-flavor sector, but also, to distinguish between new physics models. Fig. 1, reproduced from [11], illustrates a general scheme for the expected correlation between the K^+ and K_L decays under various scenarios. If the new physics has a CKM-like structure of flavor interactions, with only couplings to left-handed quark currents, the values for $\text{BR}(K^+ \rightarrow \pi^+ \nu \bar{\nu})$ and $\text{BR}(K_L \rightarrow \pi^0 \nu \bar{\nu})$ will lie along the green band in the figure. Specifically, for new physics models with minimal flavor violation, constraints from other flavor observables limit the expected size of the deviations of the BRs to within about 10% of their SM values (see, e.g., [12]). If the new physics contains only left-handed or right-handed couplings to the quark currents, it can affect $K\bar{K}$ mixing ($\Delta F = 2$) as well as $K \rightarrow \pi \nu \bar{\nu}$ decays ($\Delta F = 1$). Then, to respect constraints from the observed value of the $K\bar{K}$ mixing parameter ϵ_K , the BRs for the K^+ and K_L decays must lie on one of the two branches of the blue cross-shaped region [13]. This is characteristic of littlest-Higgs models with T parity [14] or in models with flavor-changing Z or Z' bosons and pure right-handed or left-handed couplings [2, 15]. In the most general case, if

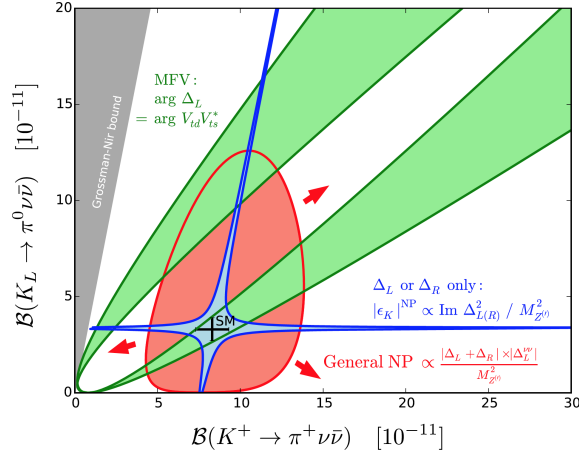


Figure 1: Scheme for BSM modifications of $K \rightarrow \pi \nu \bar{\nu}$ BRs.

the new physics has an arbitrary flavor structure and both left-handed and right-handed couplings, the constraint from ϵ_K is evaded and there is little correlation, as illustrated by the red region. This is the case for the general MSSM framework (without minimal flavor violation) [12] and in Randall-Sundrum models [16].

Like $\text{BR}(K_L \rightarrow \pi^0 \nu \bar{\nu})$, the parameter ϵ'_K also gives a direct measurement of the height of the unitarity triangle. Experimentally, $\text{Re } \epsilon'_K / \epsilon_K$ has been measured by NA48 [17] and KTeV [18], leading to the average $\text{Re } \epsilon'_K / \epsilon_K = (1.66 \pm 0.23) \times 10^{-3}$ [19]. In principle, the experimental value of $\text{Re } \epsilon'_K / \epsilon_K$ significantly constrains the value of $\text{BR}(K_L \rightarrow \pi^0 \nu \bar{\nu})$ to be expected in any given new-physics scenario. However, because of the delicate balance between the amplitudes for the hadronic matrix elements of different operators, it is difficult to perform a reliable calculation of $\text{Re } \epsilon'_K / \epsilon_K$ in the SM. In a recent breakthrough, the RBC-UKQCD Collaboration obtained the result $\text{Re } \epsilon'_K / \epsilon_K = (1.38 \pm 5.15 \pm 4.59) \times 10^{-4}$ from a lattice calculation [20], 2.1σ less than the experimental value (improvements of the analytical parts of this result have increased the significance slightly [21, 22]). Considerations from large- N_c dual QCD support the lattice result [23], but a calculation in chiral perturbation theory is in good agreement with the experimental value of $\text{Re } \epsilon'_K / \epsilon_K$ [24]. RBC-UKQCD is currently working on confirming the result and reducing both the statistical and systematic uncertainties.

With this result for $\text{Re } \epsilon'_K / \epsilon_K$ in the background, the correlation between ϵ'_K and $\text{BR}(K_L \rightarrow \pi^0 \nu \bar{\nu})$ has been examined in various SM extensions at energy scales Λ in the neighborhood of 1–10 TeV by several authors, in many cases with constraints from ϵ_K , Δm_K , and $\text{BR}(K_L \rightarrow \mu\mu)$ considered as well. The results of these studies are summarized in Table 1. As a general rule, the observation of a larger value for ϵ'_K than expected in the SM implies a suppression of $\text{BR}(K_L \rightarrow \pi^0 \nu \bar{\nu})$ to below the SM value. However, it is possible to construct models in which ϵ'_K and $\text{BR}(K_L \rightarrow \pi^0 \nu \bar{\nu})$ are simultaneously enhanced. With moderate parameter tuning (e.g., cancellation among SM and NP interference terms to the 10-20% level), $\text{BR}(K_L \rightarrow \pi^0 \nu \bar{\nu})$ may be enhanced by up to an order of magnitude.

The KOTO experiment at J-PARC is the only experiment currently pursuing the decay $K_L \rightarrow \pi^0 \nu \bar{\nu}$. KOTO continues in the tradition of the KEK experiment E391a in technique [33]. The salient features of the experiment are the use of a highly collimated, low-energy (mean momentum 2.1 GeV) “pencil” beam and very high performance hermetic calorimetry and photon vetoing. KOTO has recently obtained the limit $\text{BR}(K_L \rightarrow \pi^0 \nu \bar{\nu}) < 3 \times 10^{-9}$ (90% CL), with an expected

Model	Λ [TeV]	Effect on BR($K^+ \rightarrow \pi^+ \nu \bar{\nu}$)	Effect on BR($K_L \rightarrow \pi^0 \nu \bar{\nu}$)	Refs.
Leptoquarks, most models	1–20	Very large enhancements; mainly ruled out		[25]
Leptoquarks, U_1	1–20	+10% to +60%	+100% to +800%	[25]
Vector-like quarks	1–10	–90% to +60%	–100% to +30%	[26]
Vector-like quarks + Z'	10	–80% to +400%	–100% to 0%	[26]
Simplified modified Z , no tuning	1	–100% to +80%	–100% to –50%	[27]
General modified Z , cancellation to 20%	1	–100% to +400%	–100% to +500%	[27]
SUSY, chargino Z penguin	4–6 TeV		–100% to –40%	[28]
SUSY, gluino Z penguin	3–5.5 TeV	0% to +60%	–20% to +60%	[29]
SUSY, gluino Z penguin	10	Small effect	0% to +300%	[30]
SUSY, gluino box, tuning to 10%	1.5–3	$\pm 10\%$	$\pm 20\%$	[31]
LHT	1	$\pm 20\%$	–10% to –100%	[32]

Table 1: Effects on BRs for $K \rightarrow \pi \nu \bar{\nu}$ decays in various SM extensions, with constraints from other kaon observables, including in particular $\text{Re } \epsilon'_K / \epsilon_K$.

background of 0.42 ± 0.18 events and no candidate events observed [35]. To reach the single-event sensitivity for the SM decay, KOTO would need about a factor of 40 more data. With upgrades to the J-PARC Main Ring to gradually increase the slow-extracted (SX) beam power to 100 kW, KOTO should reach this threshold by the mid 2020s, and upgrades to the experiment planned or in progress should reduce backgrounds by a similar factor [35]. This would allow a 90% CL upper limit on the BR to be set at the 10^{-10} level, but a next-generation experiment is needed in order to actually measure the BR to test the predictions in Table 1.

KOTO has long expressed a strong intention to upgrade to O(100)-event sensitivity over the long term. To increase the kaon flux, the production angle would be decreased from 16° to 5° . This would require construction of a planned \$140M extension of the J-PARC hadron hall, which is needed for other experiments besides KOTO and is a priority for the Japan Science Council. The mean K_L momentum would be increased to 5.2 GeV. Since there are no certain prospects to increase the SX beam power beyond 100 kW, a KOTO step-2 upgrade would require the construction of a completely new detector several times larger than the present detector (in part to compensate for the effect of the increased beam momentum). There is no official step-2 proposal, timeline, or sensitivity estimate as of yet.

2 Objectives of the KLEVER project

We are designing the KLEVER experiment to use a high-energy neutral beam at the CERN SPS to achieve a sensitivity of about 60 events for the decay $K_L \rightarrow \pi^0 \nu \bar{\nu}$ at the SM BR with an S/B ratio of 1. At the SM BR, this would correspond to a relative uncertainty of about 20%, demonstrating a discrepancy with 5σ significance if the true rate is a bit more than twice or less than one-quarter of the SM rate, or with 3σ significance if the true rate is less than half of the SM rate. These scenarios are consistent with the rates predicted for many different SM extensions, as seen from Table 1.

We do not envision KLEVER as a competitor to NA62, but rather as a natural evolution of the multi-decade North Area program in kaon physics, building on the successes of NA62 and its progenitors. The KLEVER timescale is driven by the assumption that the kaon program will have advanced by the end of LHC Run 3 to the point at which the measurement of $K_L \rightarrow \pi^0 \nu \bar{\nu}$ is the natural next step. KLEVER would aim to start data taking in LHC Run 4 (2026). The layout is sketched in Figure 2. Relative to KOTO, the boost from the high-energy beam in KLEVER facilitates the rejection of background channels such as $K_L \rightarrow \pi^0 \pi^0$ by detection of the additional photons in the final state. On the other hand, the layout poses particular challenges for the design

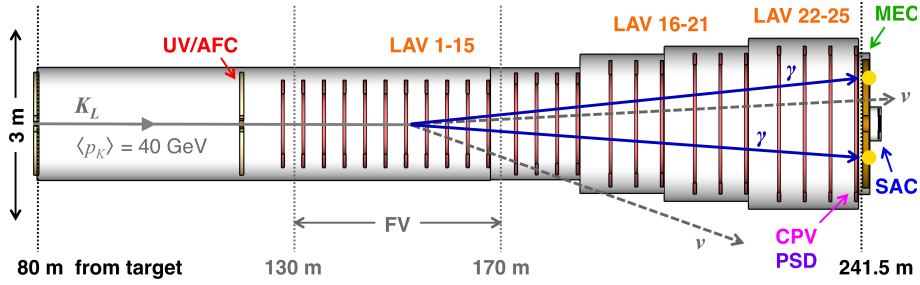


Figure 2: KLEVER experimental apparatus: upstream veto (UV) and active final collimator (AFC), large-angle photon vetoes (LAV), main electromagnetic calorimeter (MEC), small-angle calorimeter (SAC), charged particle veto (CPV), preshower detector (PSD).

of the small-angle vetoes, which must reject photons from K_L decays escaping through the beam exit amidst an intense background from soft photons and neutrons in the beam. Background from $\Lambda \rightarrow n\pi^0$ decays in the beam must also be kept under control.

3 The KLEVER experiment

3.1 Primary and secondary beams

KLEVER will make use of the 400-GeV SPS proton beam to produce a neutral secondary beam at an angle of 8 mrad with an opening angle of 0.4 mrad. The choice of production angle balances increased K_L production and higher K_L momentum at small angle with improved K_L/n and K_L/Λ ratios at larger angles. The choice of solid angle balances beam flux against the need for tight collimation for increased p_\perp constraints to reject the main background from $K_L \rightarrow \pi^0\pi^0$ with lost photons. The resulting neutral beam has a mean K_L momentum of 40 GeV, leading to an acceptance of 4% for the fiducial volume extending from 130 to 170 m downstream of the target, and a K_L yield of $2 \times 10^{-5} K_L$ per proton on target (pot). With a selection efficiency of 5%, collection of 60 SM events would require a total primary flux of 5×10^{19} pot, corresponding to an intensity of 2×10^{13} protons per pulse (ppp) under NA62-like slow-extraction conditions, with a 16.8 s spill cycle and 100 effective days of running per year. This is a six-fold increase in the primary intensity relative to NA62.

The feasibility of upgrades to the P42 beamline, TCC8 target gallery, and ECN3 experimental cavern to handle this intensity has been studied by the Conventional Beams working group in the context of the Physics Beyond Colliders initiative, and preliminary indications are positive [36, 37]:

- **Slow extraction to T4** The SPS Losses and Activation and PBC BDF/SHiP working groups have made general progress on issues related to the slow extraction of the needed intensity to the North Area, including duty cycle optimization [38]. An integrated intensity of 4×10^{19} protons/year (3×10^{19} effective pot/yr after splitter losses) can be delivered to the TCC2 targets. This would allow both KLEVER and a robust North Area fixed-target program to run concurrently. With small compromises, SHiP, KLEVER, and the North Area test beam program might be able to run concurrently, but it does not seem possible to run SHiP, KLEVER, and a robust fixed-target program all at the same time without significant compromises.

- **T4 to T10 transmission** At the T4 target, the beam will be defocused and parallel in the vertical plane, so that it mostly misses the 2 mm thick T4 target plate. The small fraction that hits the target will be sufficient to produce the H6 and H8 beams without damaging the target head. On the other hand, most of the beam will not be attenuated by T4 and the transmission to T10 could be as high as 80%.
- **Target and dump collimator (TAX)** Simulations show that the present T10 target cannot withstand an intensity of 2×10^{13} ppp. However, designs implementing concepts used in the design of the CNGS target are capable of fulfilling the requirements for the KLEVER beam. The simulations also show that the K12 TAX is already close to thermal limits during running in beam dump mode at the nominal NA62 intensity (3×10^{12} ppp). A new design is needed with optimized block materials and optimized cooling. This should be quite possible, as the TAX in the M2 beam has survived many years of operation with 1.5×10^{13} on the T6 target. The same arguments apply to the P42 TAX.
- **Containment of activated air** There was initially a concern that the air containment in the TCC8 cavern would be insufficient for KLEVER operation with the existing ventilation approach. However, the air flow inside the TCC8 target cavern was measured to be very small, rendering an expensive upgrade unnecessary.
- **Surface dose** The primary proton beam is incident on the T10 target at downward angle of 8 mrad and is further deflected downward by an additional sweeping magnet following the target. FLUKA simulations for the prompt dose on the surface above ECN3 are under way; preliminary results indicate that an adequate solution has been found for shielding the target region. Muons in the forward direction can be dealt with by a mixed mitigation strategy involving additional upstream shielding and potentially a thicker earthen shield in the downstream region, possibly in combination with better fencing around the ECN3 area.

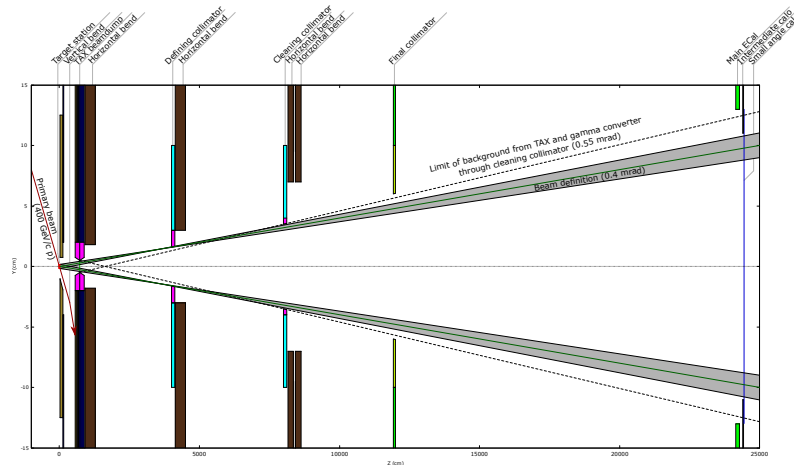


Figure 3: KLEVER neutral beamline layout as modeled in FLUKA, showing four collimation stages corresponding to dump, defining, cleaning, and final collimators. The final collimator is an active detector (AFC), built into the upstream veto. The aperture of the main calorimeter and coverage of the small-angle calorimeters is also shown.

A four-collimator neutral beamline layout for ECN3 has been developed, as illustrated in Fig. 3. The primary proton beam, sloping downwards at an angle of 8 mrad, is incident on the

T10 target (assumed to be a beryllium rod of 2 mm radius), producing the neutral beam and other secondaries. This is immediately followed by a vertical sweeping magnet that bends the protons further downward by 5.6 mrad, and a TAX dump collimator with a hole for the passage of the neutral beam. A horizontal sweeping magnet downstream of the TAX reduces the background further. A collimator at $z = 40$ m downstream of the target with $r = 16$ mm defines the beam solid angle, and a cleaning collimator at $z = 80$ m removes halo from particles interacting on the edges of the defining collimator. Both are followed by horizontal sweeping magnets. The sweeping fields have been optimized to minimize muon backgrounds. The final stage of collimation is the active final collimator (AFC) incorporated into the upstream veto (UV) at $z = 120$ m. The cleaning and final (AFC) collimators have apertures which are progressively larger than the beam acceptance, such that the former lies outside a cone from the (2 mm radius) target passing through the defining collimator, and the latter lies outside a cone from the TAX aperture passing through the cleaning collimator. The design of the beamline has been guided by FLUKA and Geant4 simulations to quantify the extent and composition of beam halo, muon backgrounds, and sweeping requirements. According to the simulations, for an intensity of 2×10^{13} ppp and an effective spill length of 3 s, there are 140 MHz of K_L in the beam and 440 MHz of neutrons [39]. An oriented tungsten crystal in the center of the TAX converts the vast majority of the photons in the beam into e^+e^- pairs, which are swept away, but 40 MHz of photons with energy greater than 5 GeV remain. As noted below, a crystal converter is used to maximize the transparency to neutral hadrons at a given thickness in radiation lengths ($9.4X_0$).

3.2 Detector subsystems

Because the experimental challenges involved in the measurement of $K_L \rightarrow \pi^0 \nu \bar{\nu}$, and in particular, the very high efficiency required for the photon veto systems, most of the subdetector systems for KLEVER will have to be newly constructed.

Main electromagnetic calorimeter (MEC) Early studies indicated that the NA48 liquid-krypton calorimeter (LKr) [40] currently used in NA62 could be reused as the MEC for reconstruction of the π^0 for signal events and rejection of events with additional photons. Indeed, the efficiency and energy resolution of the LKr appear to be satisfactory for KLEVER. However, the LKr time resolution would be a major liability. The LKr would measure the event time in KLEVER with 500 ps resolution, while the total rate of accidental vetoes (dominated by the rate from beam photons interacting in the SAC) could be 100 MHz. The LKr time resolution might be improved via a comprehensive readout upgrade, but concerns about the service life of the LKr would remain, and the size of the inner bore would limit the beam solid angle and hence kaon flux.

We are investigating the possibility of replacing the LKr with a shashlyk-based MEC patterned on the PANDA FS calorimeter (in turn, based on the KOPIO calorimeter [41]), with 110×110 mm modules, lead absorber thickness of 0.275 mm, and scintillator thickness of 1.5 mm, read out by silicon photomultipliers via 1-mm diameter WLS fibers. Stochastic energy and time resolutions of better than $\sigma_E/E = 2\%/\sqrt{E}$ and $\sigma_t = 72$ ps/ \sqrt{E} were obtained with this design in KOPIO tests. We envisage a shashlyk design incorporating “spy tiles”, consisting of 10-mm thick scintillator bricks incorporated into the shashlyk stack but optically isolated from it, read out by separate WLS fibers. The spy tiles are located at key points in the longitudinal shower development: near the front of the stack, near shower maximum, and in the shower tail. This provides longitudinal sampling of the shower development, resulting in additional information for γ/n separation. A first test of this concept was carried out with a prototype detector at Protvino in April 2018.

Upstream veto (UV) and active final collimator (AFC) The upstream veto (UV) rejects $K_L \rightarrow \pi^0\pi^0$ decays in the 40 m upstream of the fiducial volume where there are no large-angle photon vetoes. This is necessary, since it is possible for $K_L \rightarrow \pi^0\pi^0$ decays in this region to place two photons on the fiducially accepted area of the MEC ($r > 35$ cm). The UV is a shashlyk calorimeter with the same basic structure as the MEC (without the spy tiles).

The active final collimator (AFC) is inserted into a 100-mm hole in center of the UV. The AFC is a LYSO collar counter with angled inner surfaces to provide the last stage of beam collimation while vetoing photons from K_L that decay in transit through the collimator itself. The collar is made of 24 crystals of trapezoidal cross section, forming a detector with an inner radius of 60 mm. The UV and AFC are both 800 mm in depth. The maximum crystal length for a practical AFC design is about 250 mm, so the detector consists of 3 or 4 longitudinal segments. The crystals are read out on the back side with two avalanche photodiodes (APDs). These devices couple well with LYSO and offer high quantum efficiency, simple signal and HV management. Studies indicate that a light yield in excess of 4000 p.e./MeV should be easy to achieve.

Large-angle photon vetoes Because of the boost from the high-energy beam, it is sufficient for the large-angle photon vetoes (LAVs) to cover polar angles out to 100 mrad. The detectors themselves must have inefficiencies of less than a few 10^{-4} down to at least 100 MeV, so the current NA62 LAVs based on the OPAL lead glass cannot be reused. The 25 new LAV detectors for KLEVER are lead/scintillating-tile sampling calorimeters with wavelength-shifting fiber readout, based on the CKM VVS design [42]. Extensive experience with this type of detector (including in prototype tests for NA62) demonstrates that the low-energy photon detection efficiency will be sufficient for KLEVER [43, 44, 45].

Small-angle calorimeter The small-angle calorimeter (SAC) sits directly in the neutral beam and must reject photons from K_L decays that would otherwise escape via the downstream beam exit. The veto efficiency required is not intrinsically daunting (inefficiency $< 1\%$ for $5 \text{ GeV} < E_\gamma < 30 \text{ GeV}$ and $< 10^{-4}$ for $E_\gamma > 30 \text{ GeV}$; the SAC can be blind for $E_\gamma < 5 \text{ GeV}$), but must be attained while maintaining insensitivity to more than 500 MHz of neutral hadrons in the beam. In addition, the SAC must have good longitudinal and transverse segmentation to provide γ/n discrimination. In order to keep the false veto rate from accidental coincidence of beam neutrons to an acceptable level ($< 10 \text{ MHz}$), and assuming that about 25% of the beam neutrons leave signals above threshold in the SAC, topological information from the SAC must allow residual neutron interactions to be identified with 90% efficiency while maintaining 99% detection efficiency for photons with $5 \text{ GeV} < E_\gamma < 30 \text{ GeV}$.

An intriguing possibility for the construction of an instrument that is sensitive to photons and blind to hadrons is to use a compact Si-W sampling calorimeter with crystalline tungsten tiles as the absorber material, since coherent interactions of high-energy photons with a crystal lattice can lead to increased rates of pair conversion relative to those obtained with amorphous materials [46, 47, 48]. The effect is dependent on photon energy and incident angle; in the case of KLEVER, one might hope to decrease the ratio X_0/λ_{int} by a factor of 2–3. The same effect could be used to efficiently convert high-energy photons in the neutral beam to e^+e^- pairs at the TAX for subsequent sweeping, thereby allowing the use of a thinner converter to minimize the scattering of hadrons from the beam. Both concepts were tested in summer 2018 in the SPS H2 beam line, in a joint effort together with the AXIAL collaboration. In these tests, a beam of tagged photons with energies of up to 80 GeV was obtained from a 120-GeV electron beam; interactions of the beam with crystalline tungsten samples of 2 mm and 10 mm thick were studied as a function of photon

energy and angle of incidence with detectors just downstream of the samples to measure charged multiplicity and forward energy. While the data are still under analysis, the initial results show a significant increase for both samples in the probability for electromagnetic interactions when the crystal axis is aligned with the beam, corresponding to the expected shortening of the radiation length, with a somewhat smaller effect in the (lower-quality) thicker crystal counterbalanced by a larger angular range over which the effect is observed (a few mrad vs. about 1 mrad).

Charged-particle rejection For the rejection of charged particles, K_{e3} is a benchmark channel because of its large BR and because the final state electron can be mistaken for a photon. Simulations indicate that the needed rejection can be achieved with two planes of charged-particle veto (CPV) each providing 99.5% detection efficiency, supplemented by the μ^\pm and π^\pm recognition capabilities of the MEC (assumed in this case to be equal to those of the LKr) and the current NA62 hadronic calorimeters and muon vetoes, which could be reused in KLEVER. The CPVs are positioned ~ 3 m upstream of the MEC and are assumed to be constructed out of thin scintillator tiles. In thicker scintillation hodoscopes, the detection inefficiency arises mainly from the gaps between scintillators. For KLEVER, the scintillators will be only 5 mm thick (1.2% X0), and the design will be carefully optimized to avoid insensitive gaps.

Preshower detector The PSD measures the directions for photons incident on the MEC. Without the PSD, the z -position of the π^0 decay vertex can only be reconstructed by assuming that two clusters on the MEC are indeed photons from the decay of a single π^0 . With the PSD, a vertex can be reconstructed by projecting the photon trajectories to the beamline. The invariant mass is then an independent quantity, and $K_L \rightarrow \pi^0\pi^0$ decays with mispaired photons can be efficiently rejected. The vertex can be reconstructed using a single photon and the constraint from the nominal beam axis. Simulations show that with $0.5X_0$ of converter (corresponding to a probability of at least one conversion of 50%) and two tracking planes with a spatial resolution of $100 \mu\text{m}$, placed 50 cm apart, the mass resolution is about 20 MeV and the vertex position resolution is about 10 m. The tracking detectors must cover a surface of about 5 m^2 with minimal material. Micropattern gas detector (MPGD) technology seems perfectly suited for the PSD. Information from the PSD will be used for bifurcation studies of the background and for the selection of control samples, as well as in signal selection.

3.3 Simulation and performance

Simulations of the experiment carried out with fast-simulation techniques (idealized geometry, parameterized detector response, etc.) show that the target sensitivity is achievable (60 SM events with $S/B = 1$). Background channels considered at high simulation statistics include $K_L \rightarrow \pi^0\pi^0$ (including events with reconstructed photons from different π^0 s and events with overlapping photons on the MEC), $K_L \rightarrow 3\pi^0$, and $K_L \rightarrow \gamma\gamma$. Fig. 4 illustrates the scheme for differentiating signal events from $K_L \rightarrow \pi^0\pi^0$ background. Events with exactly two photons on the MEC and no other activity in the detector are selected. The clusters on the MEC from both photons must also be more than 35 cm from the beam axis (this helps to increase the rejection for events with overlapping clusters). If one or both photons convert in the PSD, the reconstructed vertex position must be inside the fiducial volume. The plots show the distributions of the events satisfying these minimal criteria in the plane of p_\perp vs. z_{rec} for the π^0 , where the distance from the π^0 to the MEC is obtained from the transverse separation of the two photon clusters, assuming that they come from a π^0 ($M_{\gamma\gamma} = m_{\pi^0}$). This scheme is far from final and there is room for improvement with

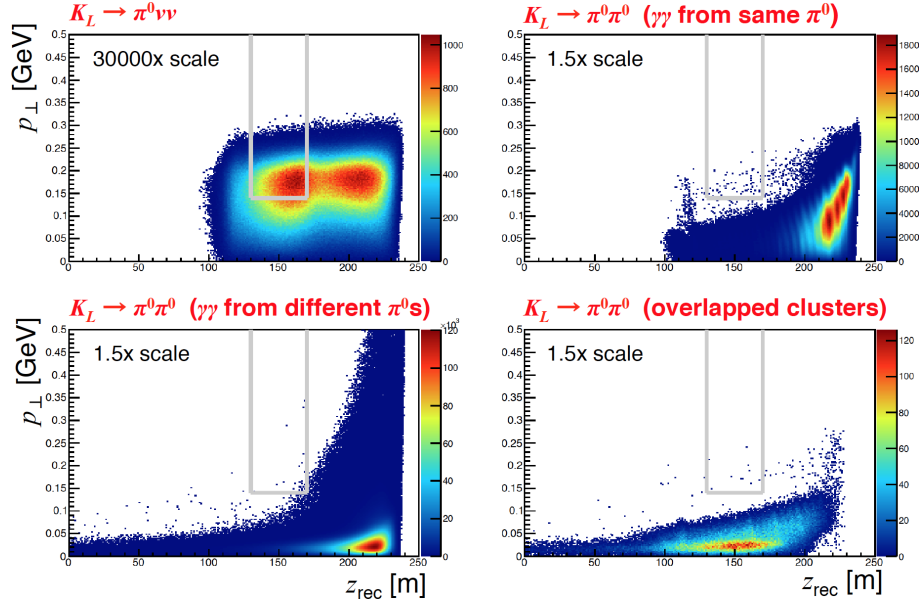


Figure 4: Distributions of events in plane of $(z_{\text{rec}}, p_{\perp})$ after basic event selection cuts, from fast MC simulation, for $K_L \rightarrow \pi^0 \nu \bar{\nu}$ events (top left) and for $K_L \rightarrow \pi^0 \pi^0$ events with two photons from the same π^0 (top right), two photons from different π^0 s (bottom left), and with two or more indistinguishable overlapping photon clusters (bottom right).

a multivariate analysis, but it does demonstrate that it should be possible to obtain $S/B \sim 1$ with respect to other K_L decays. Background from $\Lambda \rightarrow n\pi^0$ and from decays with charged particles is assumed to be eliminated on the basis of studies with more limited statistics. This background is reduced by several orders of magnitude by the 130-m length from the target to the fiducial volume and the choice of production angle, which is carefully optimized to balance K_L flux against the need to keep the Λ momentum spectrum soft. Residual background from $\Lambda \rightarrow n\pi^0$ ($p^* = 104$ MeV) can be effectively eliminated by cuts on p_{\perp} and in the θ vs. p plane for the π^0 .

An effort is underway to develop a comprehensive simulation and use it to validate the results obtained so far. Of particular note, backgrounds from radiative K_L decays, cascading hyperon decays, and beam-gas interactions remain to be studied, and the neutral-beam halo from our more detailed FLUKA simulations needs to be incorporated into the simulation of the experiment. While mitigation of potential background contributions from one or more of these sources might ultimately require specific modifications to the experimental setup, we expect this task to be straightforward in comparison to the primary challenges from $K_L \rightarrow \pi^0 \pi^0$ and $\Lambda \rightarrow n\pi^0$.

3.4 Trigger, data acquisition, and readout

Preliminary studies indicate that the hit and event rates on most of the detectors are on the order of a few tens of MHz, a few times larger than in NA62, with the notable exception of the SAC, which will require an innovative readout solution to handle rates of 100 MHz. Digitization of the signals from the KLEVER detectors with FADCs at high frequency (up to 1 GHz) would help to efficiently veto background events without inducing dead time. For the SAC, this is strictly necessary, since the signal duration will be long compared to the mean interval between events

on a single channel. Detailed signal analysis may also assist with particle identification and discrimination of uncorrelated background, for example, from muon halo.

A free-running readout system would have various advantages: there are no issues with latency, data are not buffered in the front-end and thus not susceptible to radiation-induced corruption, and above all, data selection is performed by software, leading to a powerful and flexible trigger system that can in principle implement the full offline analysis criteria, with no emulation required. On the other hand, a free-running, continuously digitizing readout implies very challenging data rates. Assuming 100 MHz of interactions in the SAC and current hit multiplicity and event size estimates, the data flow from the SAC alone would be 100 GB/s.

A possible scheme for the readout system includes a low-level front-end layer (L0) in which signals are digitized and timestamped using TDCs with 100 ps precision, and then transferred via a radiation hard link, for example, via optical GBT link, to a readout board such as the PCIe40 board under development for LHCb or the FELIX board under development by ATLAS. The first layer of data selection (L1) may be implemented on this board. For example, methods for the γ/n discrimination in the SAC or cluster finding algorithms for the MEC may be implemented. The output is written directly into the memory of the host PC, which then routes the data to the online PC farm. Once again, the data is received on a readout board for event building. where the data may be preprocessed on GPUs or FPGA accelerators before being loaded into the PC memory. The specific solutions discussed here are intended as examples to demonstrate that a readout system with the needed requirements is within reach. Further evolution (including KLEVER R&D) is expected before actual solutions are chosen.

4 Outlook

KLEVER would aim to start data taking in LHC Run 4 (2026). Assuming a delivered proton intensity of 10^{19} pot/yr, collection of 60 SM events would require five years of data taking. To be ready for the 2026 start date, detector construction would have to begin by 2021 and be ready for installation by 2025, leaving three years from the present for design consolidation and R&D. An Expression of Interest to the SPSC is in preparation.

The KLEVER project builds on a CERN tradition of groundbreaking experiments in kaon physics, following on the successes of NA31, NA48, NA48/2, and NA62. Many institutes currently participating in NA62 have expressed support for and interest in the KLEVER project. Successfully carrying out the KLEVER experimental program will require the involvement of new institutions and groups, and we are actively seeking to expand the collaboration at present.

References

- [1] A. J. Buras, D. Buttazzo, J. Girrbach-Noe and R. Knegjens, *JHEP* **1511** (2015) 033 [arXiv:1503.02693 [hep-ph]]
- [2] A. J. Buras, D. Buttazzo, J. Girrbach-Noe and R. Knegjens, *JHEP* **1411** (2014) 121 [arXiv:1408.0728 [hep-ph]]
- [3] S. Bifani, S. Descotes-Genon, A. Romero Vidal and M. H. Schune, arXiv:1809.06229 [hep-ex]
- [4] M. Bordone, D. Buttazzo, G. Isidori and J. Monnard, *Eur. Phys. J. C* **77** (2017) no.9, 618 [arXiv:1705.10729 [hep-ph]]
- [5] D. Buttazzo, A. Greljo, G. Isidori and D. Marzocca, *JHEP* **1711** (2017) 044 [arXiv:1706.07808 [hep-ph]]
- [6] S. Fajfer, N. Košnik and L. Vale Silva, *Eur. Phys. J. C* **78** (2018) 275 [arXiv:1802.00786 [hep-ph]]
- [7] A. V. Artamonov *et al.* [BNL-E949 Collaboration], *Phys. Rev. D* **79** (2009) 092004
- [8] E. Cortina Gil *et al.* [NA62 Collaboration], *JINST* **12** (2017) P05025 [arXiv:1703.08501 [physics.ins-det]]
- [9] E. Cortina Gil *et al.* [NA62 Collaboration], arXiv:1811.08508 [hep-ex].
- [10] Y. Grossman and Y. Nir, *Phys. Lett. B* **398** (1997) 163
- [11] A. J. Buras, D. Buttazzo and R. Knegjens, *JHEP* **1511** (2015) 166 [arXiv:1507.08672 [hep-ph]]

- [12] G. Isidori, F. Mescia, P. Paradisi, C. Smith and S. Trine, *JHEP* **0608** (2006) 064
- [13] M. Blanke, *Acta Phys. Polon. B* **41** (2010) 127
- [14] M. Blanke, A. J. Buras, B. Duling, S. Recksiegel and C. Tarantino, *Acta Phys. Polon. B* **41** (2010) 657
- [15] A. J. Buras, F. De Fazio and J. Girrbach, *JHEP* **1302** (2013) 116
- [16] M. Blanke, A. J. Buras, B. Duling, K. Gemmler and S. Gori, *JHEP* **0903** (2009) 108
- [17] J. R. Batley *et al.* [NA48 Collaboration], *Phys. Lett. B* **544** (2002) 97
- [18] E. Abouzaid *et al.* [KTeV Collaboration], *Phys. Rev. D* **83** (2011) 092001
- [19] M. Tanabashi *et al.* [Particle Data Group], *Phys. Rev. D* **98** (2018) 030001
- [20] Z. Bai *et al.* [RBC and UKQCD Collaborations], *Phys. Rev. Lett.* **115** (2015) 212001
- [21] A. J. Buras, M. Gorbahn, S. Jäger and M. Jamin, *JHEP* **1511** (2015) 202
- [22] T. Kitahara, U. Nierste and P. Tremper, *JHEP* **1612** (2016) 078
- [23] A. J. Buras, *Acta Phys. Polon. B* **49** (2018) 1043
- [24] H. Gisbert and A. Pich, *Rept. Prog. Phys.* **81** (2018) 076201
- [25] C. Bobeth and A. J. Buras, *JHEP* **1802** (2018) 101
- [26] C. Bobeth, A. J. Buras, A. Celis and M. Jung, *JHEP* **1704** (2017) 079
- [27] M. Endo, T. Kitahara, S. Mishima and K. Yamamoto, *Phys. Lett. B* **771** (2017) 37
- [28] M. Endo, S. Mishima, D. Ueda and K. Yamamoto, *Phys. Lett. B* **762** (2016) 493
- [29] M. Endo, T. Goto, T. Kitahara, S. Mishima, D. Ueda and K. Yamamoto, *JHEP* **1804** (2018) 019
- [30] M. Tanimoto and K. Yamamoto, *PTEP* **2016** (2016) 123B02
- [31] A. Crivellin, G. D'Ambrosio, T. Kitahara and U. Nierste, *Phys. Rev. D* **96** (2017) 015023
- [32] M. Blanke, A. J. Buras and S. Recksiegel, *Eur. Phys. J. C* **76** (2016) 182
- [33] J. K. Ahn *et al.* [E391a Collaboration], *Phys. Rev. Lett.* **100** (2008) 201802
- [34] J. K. Ahn *et al.* [KOTO Collaboration], arXiv:1810.09655 [hep-ex].
- [35] T. Yamanaka, presentation at the 26th J-PARC Program Advisory Committee, 18 July 2018, <https://kds.kek.jp/indico/event/28286/contribution/11/material/slides/1.pdf>
- [36] D. Banerjee *et al.* for the PBC Conventional Beams Working Group, CERN-PBC-NOTES-2018-005
- [37] L. Gagnon *et al.*, for the PBC Conventional Beams Working Group, CERN-PBC-REPORT-2018-002
- [38] H. Bartosik *et al.*, CERN-ACC-NOTE-2018-0082
- [39] M. van Dijk and M. Rosenthal, CERN-PBC-NOTES-2018-002/CERN-ACC-NOTE-2018-066/KLEVER-PUB-18-01
- [40] V. Fanti *et al.* [NA48 Collaboration], *Nucl. Instrum. Meth. A* **574** (2007) 433
- [41] G. S. Atoian *et al.*, *Nucl. Instrum. Meth. A* **584** (2008) 291 [arXiv:0709.4514 [physics.ins-det]]
- [42] E. Ramberg, P. Cooper and R. Tschirhart, *IEEE Trans. Nucl. Sci.* **51** (2004) 2201
- [43] M. S. Atiya *et al.*, *Nucl. Instrum. Meth. A* **321** (1992) 129
- [44] J. R. Comfort *et al.* (KOPIO Project), Conceptual Design Report, April 2005
- [45] F. Ambrosino *et al.*, Proceedings, 2007 IEEE Nuclear Science Symposium and Medical Imaging Conference: Honolulu, Hawaii, 28 October-3 November 2007, p. 57-64 [arXiv:0711.3398 [physics.ins-det]]
- [46] J. F. Bak *et al.*, *Phys. Lett. B* **202** (1988) 615
- [47] J. C. Kimball and N. Cue, *Phys. Rept.* **125** (1985) 69
- [48] V. G. Baryshevsky and V. V. Tikhomirov, *Sov. Phys. Usp.* **32** (1989) 1013 [*Usp. Fiz. Nauk* **159** (1989) 529]